CHEMISTRY & SUSTAINABILITY
CHEMSUSCHEM
ENERGY & MATERIALS

Accepted Article

Title: Towards Sustainable H2 Production: Rational Design of Hydrophobic Triphenylamine-based Dyes for Sensitized Ethanol Photoreforming

Authors: Alessio Dessì, Matteo Monai, Matteo Bessi, Tiziano Montini, Massimo Calamante, Alessandro Mordini, Gianna Reginato, Cosimo Trono, Paolo Fornasiero, and Lorenzo Zani

To be cited as: *ChemSusChem* 10.1002/cssc.201701707

Link to VoR: http://dx.doi.org/10.1002/cssc.201701707

A Journal of ChemPubSoc Europe

WILEY-VCH www.chemsuschem.org

Towards Sustainable H_2 Production: Rational Design of Hydrophobic Triphenylamine-based Dyes for Sensitized Ethanol Photoreforming

Alessio Dessì,[a],§ Matteo Monai,[b],§ Matteo Bessi,[a,c],§ Tiziano Montini,[b] Massimo Calamante,[a] Alessandro Mordini,[a] Gianna Reginato,[a] Cosimo Trono,[d] Paolo Fornasiero,[b],* Lorenzo Zani[a],*

Abstract: Donor-acceptor dyes are a well-established class of photosensitizers, used to enhance visible light harvesting in solar cells and in direct photocatalytic reactions, such as H_2 production by photoreforming of sacrificial electron donors (SEDs). Amines - typically triethanolamine (TEOA) - are commonly employed as SEDs in such reactions. Dye-sensitized photoreforming of more sustainable, biomass-derived alcohols, on the other hand, was only recently reported using methanol as the electron donor. In this work, several rationally designed donor-acceptor dyes were used as sensitizers in H_2 photocatalytic production, comparing the efficiency of TEOA and EtOH as SEDs. In particular, the effect of hydrophobic chains in the spacer and/or the donor unit of the dyes was systematically studied. The H_2 production rates were higher when TEOA was used as SED, while the activity trends were dependent on the SED used. With TEOA, the best performance was obtained using a sensitizer (**AD418**) endowed with just one bulky hydrophobic moiety, propylenedioxythiophene (ProDOT), placed on the spacer unit. In the case of EtOH, the best performing sensitizers (**TTZ4-5**) were the ones featuring a thiazolo[5,4-*d*]thiazole internal unit, needed for enhancing light harvesting, and carrying alkyl chains on both the donor part and the spacer unit. The results are discussed in terms of reaction mechanism, interaction with SED and structural/ electrochemical properties of the sensitizers.

Introduction

Hydrogen is an essential chemical for nowadays most important industrial and manufacturing processes, ranging from ammonia and methanol synthesis to fuel cells power generation and food processing. However, despite the great efforts made in the last decades, sustainable H_2 production from low-carbon or renewable energies remains challenging and will require large-scale changes to our energy systems.[1]

While photocatalytic water splitting is the dream reaction for clean H_2 production, its low efficiency limits its feasibility. Photoreforming of renewable feedstocks, in which an organic compound acts as a sacrificial electron donor (SED), bypassing the water oxidation reaction, is a valid alternative. In this field, titanium dioxide, TiO_2, is the most investigated material, because it is cheap, nontoxic, chemically and biologically inert, and photo-stable. In particular, when coupled with appropriate metal co-catalysts such as, among others, Pt, Pd, Au or Ni, TiO_2 performs very well in many photocatalytic reactions,[2] and has been demonstrated to efficiently mediate photoreforming of biomass-derived SEDs (glucose, wood hydrolysate, simple alcohols).[3-10] However, TiO_2 does not absorb visible light, because of its large band gap (~3.2 eV, depending on polymorph and nanostructure), so that only a narrow, UV (Ultraviolet) portion of the solar spectrum can contribute to electron excitation from its valence band (VB) to the conduction band (CB). Among the many strategies to enhance light harvesting, coupling TiO_2 with visible light-absorbing moieties such as colored dyes is a well-established approach, which is largely employed in the field of solar cells (*i.e.* dye-sensitized solar cells (DSSCs)).[11] The dye acts as a photosensitizer, or antenna, whose main purposes are to efficiently absorb Vis light and trigger the remaining steps of the hydrogen production process by electron injection into TiO_2 CB. Obviously, the photosensitizer must also be stable in the working conditions, *i.e.* under continuous irradiation over long periods.

Figure 1 illustrates the working mechanism of a dye-sensitized Pt/TiO_2 photocatalyst for H_2 production, summarized in Equations (1-6).[12] First, the dye absorbs a photon and enters an excited state (1). Electron injection into the CB of TiO_2 results in charge separation (2). The regeneration of the oxidized dye occurs by oxidation of the SED agent (3). Notably, no holes are generated in the semiconductor since TiO_2 cannot generate photoelectrons under visible light illumination, so the electron transfer must occur between the SED and the excited dye for the photocatalytic cycle to be completed. Electrons are then transferred from TiO_2 to Pt(0) nanoparticles adsorbed on the TiO_2 surface, on which protons are reduced to molecular hydrogen (4). This ideal process can be

---

[a] Dr. A. Dessì, M. Bessi, Dr. M. Calamante, Dr. A. Mordini, Dr. G. Reginato, Dr. L. Zani
Institute for the Chemistry of Organometallic Compounds (ICCOM-CNR)
Via Madonna del Piano 10, 50019 Sesto Fiorentino, Italy
E-mail: lorenzo.zani@iccom.cnr.it
[b] Dr. M. Monai, Dr. T. Montini, Prof. P. Fornasiero
Department of Chemical and Pharmaceutical Sciences, ICCOM-CNR Trieste Research Unit and INSTM Research Unit, University of Trieste
via L. Giorgieri 1, 34127 Trieste, Italy
E-mail: pfornasiero@units.it
[c] M. Bessi
Department of Biotechnology, Chemistry and Pharmacy
University of Siena
Via A. Moro 2, 53100 Siena, Italy
[d] Dr. C. Trono
Institute of Applied Physics "Nello Carrara" (IFAC-CNR)
Via Madonna del Piano 10, 50019 Sesto Fiorentino, Italy

§ These authors contributed equally to this work.

Supporting information for this article is given via a link at the end of the document.

hindered by some unwanted events, such as: the relaxation of the dye to its ground state before electron injection into the CB of the semiconductor (5) and hole–electron recombination between TiO_2 and dye (6), which competes with the H_2 generation (4) and dye regeneration (3) steps.

$$Pt/TiO_2/Dye \xrightarrow{h\nu} Pt/TiO_2/Dye^* \tag{1}$$

$$Pt/TiO_2/Dye^* \rightarrow Pt/TiO_2(e^-)/Dye^{+\cdot} \tag{2}$$

$$Pt/TiO_2(e^-)/Dye^{+\cdot} + SED \rightarrow Pt/TiO_2(e^-)/Dye + SED^+ \tag{3}$$

$$Pt/TiO_2(e^-)/Dye + H^+ \rightarrow Pt/TiO_2/Dye + \frac{1}{2}H_2 \tag{4}$$

$$Pt/TiO_2/Dye^* \rightarrow Pt/TiO_2/Dye + h\nu \tag{5}$$

$$Pt/TiO_2(e^-)/Dye^{+\cdot} \rightarrow Pt/TiO_2/Dye \tag{6}$$

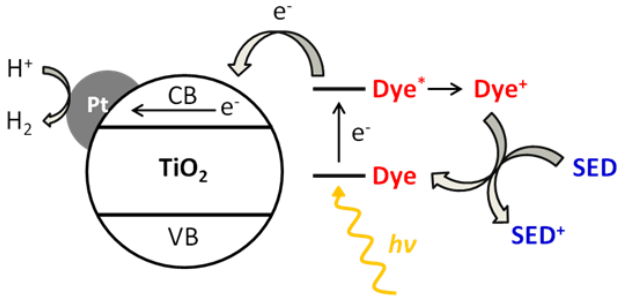

Figure 1. Graphical representation of the working mechanism for H_2 production over dye-sensitized Pt/TiO_2 photocatalysts.

In most cases, the organic sensitizers employed are characterized by a donor-π-acceptor (D-π-A) architecture,[12] in which the HOMO is located on the donor core and the LUMO on the acceptor end-group. Upon irradiation, an electron is promoted from the HOMO to the LUMO of the dye, corresponding to an intramolecular charge transfer (ICT) transition. Once in its excited state, electron transfer from the LUMO of the sensitizer to the conduction band of TiO_2 takes place, thus triggering the photocatalytic cycle.

The nature of the SED plays an important role in photocatalytic reactions kinetics as well. The most commonly used electron donors in dye-sensitized photocatalysis are TEOA and EDTA for H_2 production, while redox couples such as IO_3^-/I^- and Fe^{2+}/Fe^{3+} are used for water splitting.[13] On the other hand, among alcohols, a very well-known class of SEDs in photocatalysis,[14] only MeOH has been used in dye-sensitized systems.[12,15] In particular, to the best of our knowledge, ethanol was never reported as SED for dye-sensitized photocatalysts, despite its relevance as sustainable feedstock, which can be cost-efficiently produced from renewable biomasses.[16] Finally, it must be taken into account that dye-sensitized systems are sensitive not only to the relative energy levels of the dye and SED, but also to the electron transfer kinetics that are related to the interactions among the dye molecules, the semiconductor, and the SED.[17] These interactions can be tuned by a rational molecular engineering of the organic sensitizer, leading to an enhancement of the photocatalytic performance with a particular SED.

For instance, it has been recently shown[18,19] that hydrophilic substituents placed on the terminal portion of organic dyes can enhance their affinity towards the aqueous environment used in the experiments, thus improving catalytic performances by favoring the interaction with reactants in solution. On the other hand, positioning hydrophobic side chains on dye molecules could also have a positive impact on H_2 production, since they should prevent adsorption of water on TiO_2 surface, reducing the possibility of dye deactivation / desorption from the semiconductor. Furthermore, in analogy to what happens in dye-sensitized solar cells,[11] hydrophobic side chains should also be able to suppress undesirable dye aggregation and increase the stability of oxidized dyes by preventing fast charge recombination between them and electrons in the conduction band of TiO_2, as well as protecting them from the attack of nucleophilic species present in the reaction environment.

Some studies concerning the use of dyes endowed with hydrophobic substituents have already been published,[20-23] and in a few cases it was actually shown that elongation of the alkyl chains had a positive influence on hydrogen generation.[24,25] Nevertheless, a specific investigation on the effect that a different positioning of the lipophilic side chains could have on dye properties, and therefore on photocatalytic activity, was not reported so far. In this work, we decided to test a series of D-π-A dyes having hydrophobic side chains in different positions of their molecular scaffold, presuming that such design could influence both the reduction of dye desorption and the anti-aggregation / recombination effect, and, at the same time, still allow SED molecules dissolved in the aqueous environment to interact with the oxidized dye. To do that, alkyl chains were placed on the internal, conjugated section of the sensitizers and/or on their donor part. The organic dyes were tested as sensitizers in H_2 photocatalytic using either TEOA or EtOH as SEDs, in order to assess the possibility to produce hydrogen employing a renewable and nontoxic reducing agent.

Results and Discussion

A series of D-π-A organic dyes having a triphenylamine donor unit (Figure 2) was synthesized and tested in the photo-sensitization of Pt/TiO_2 for the photocatalytic production of H_2. The simple organic dye **D5** (Figure 2) was used as a reference and systematically modified in order to get insight in structure-activity and stability relations. Compound **D5** is well-known for its use in DSSCs[26] and has also been applied to sensitize $Pt\text{-}TiO_2$ photocatalysts.[21] With the aim of evaluating the influence of introducing hydrophobic groups in different positions of the molecule, the performances of **D5** were compared with those of two derivate dyes: the previously reported sensitizer **DF15**, having two hexyloxy chains on its terminal triarylamine group,[27]

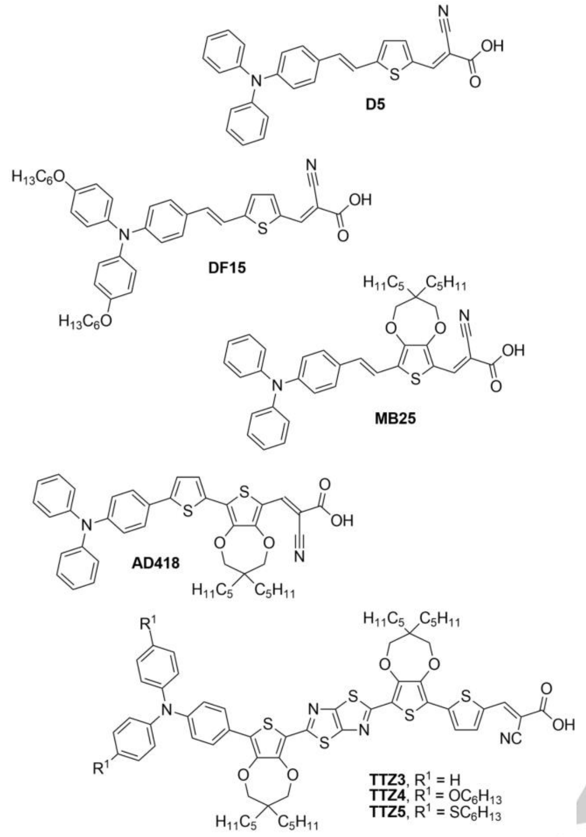

Figure 2. Structure of the dyes investigated in this study.

and the newly synthesized dye **MB25**, having the intermediate thiophene ring replaced by a propylenedioxythiophene (ProDOT) moiety, bearing two *n*-pentyl chains (Figure 2). Such substitution was aimed at favoring dye disaggregation and enhancing the shielding effect of the TiO_2 surface, as the alkyl chains on the ProDOT group should stick out of the molecular plane due to the tetrahedral geometry of its quaternary carbon atom.[28] Considering that **D5** has a relatively large HOMO-LUMO-gap with a low-lying HOMO (Table 1), we anticipated that light-harvesting properties could also be improved by introducing the alkyl chains as a part of electron-donating alkoxy groups. Finally, in order to study the effect of the spacer moiety, dye **AD418**, in which the double bond was replaced by a thiophene ring, was also prepared and tested together with known, more elaborated dyes **TTZ3-5**. **TTZ** dyes have an electron withdrawing thiazolo[5,4-*d*]thiazole moiety in the π-scaffold and are characterized by long term stability and by very high molar extinction coefficients, which has made them especially suitable for the fabrication of thin-layer dye-sensitized solar cells (Figure 2).[28,29] **TTZ4** and **TTZ5** carry hydrophobic chains both on the central scaffold and on the donor moiety, while **TTZ3** only has chains on its central scaffold.

The synthesis of compound **MB25** is outlined in Scheme 1. We anticipated that its conjugated scaffold could be generated by a diastereoselective Horner-Wadsworth-Emmons (HWE) reaction, whose application required access to diethylphosphonate **4**. To this end, ProDOT aldehyde **1**[30] was first reduced to the corresponding primary alcohol **2** using sodium borohydride in a methanol / dichloromethane mixture. Compound **2** was then converted to the corresponding chloride **3** by reaction with $SOCl_2$ in the presence of triethylamine and catalytic DMAP, and the

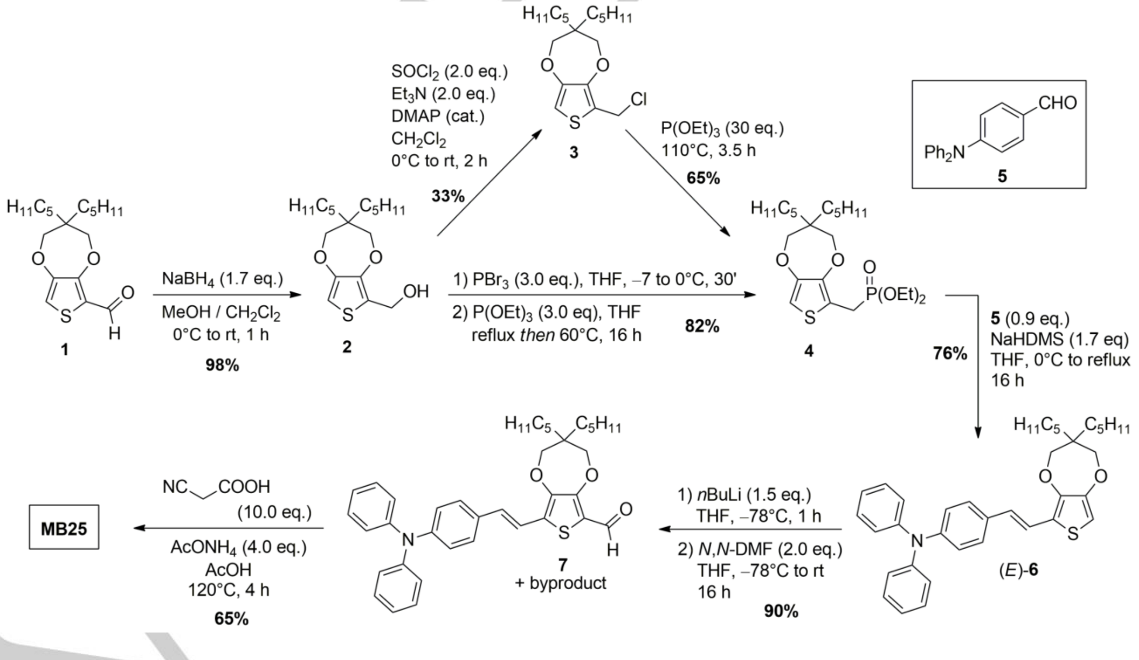

Scheme 1. Synthesis of compound **MB25** starting from ProDOT aldehyde **1**.

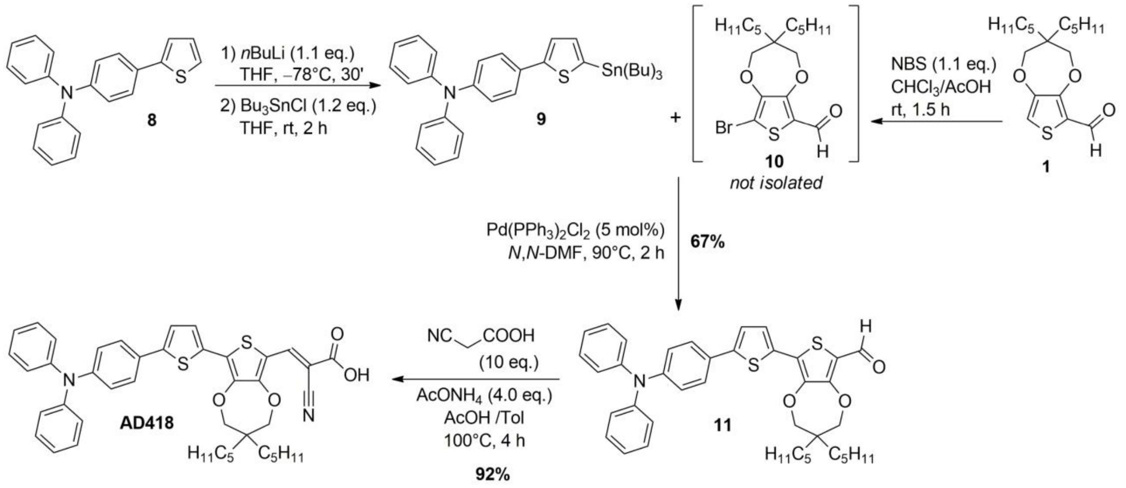

Scheme 2. Synthesis of compound **AD418** starting from ProDOT aldehyde **1** and substituted thiophene **8**.

chloride was then reacted with triethylphosphite, under typical Michaelis-Arbuzov conditions, to give phosphonate **4**, however in low yield (21%, over two steps). Since this result was mostly due to the difficult isolation of compound **3**, which underwent extensive decomposition during chromatographic purification, we decided to improve the process generating the halide in a single-pot procedure. Thus, a THF solution of alcohol **2** was treated with PBr_3 at 0 °C for 30 min to obtain the corresponding bromide, which was then reacted in situ with $P(OEt)_3$ at reflux overnight. In these conditions compound **4** was more conveniently prepared in 82% overall yield. Phosphonate **4** was then reacted with 4-(diphenylamino)benzaldehyde (**5**) in the presence of a base, to obtain disubstituted olefin **6**. While employment of *t*-BuONa and NaH allowed recovery of the product only in moderate yields (43-50%, respectively), use of 1.7 eq. of NaHMDS proved more efficient, leading to selective formation of olefin (*E*)-**6** in 76% yield (as demonstrated by analysis of the ^{1}H-NMR coupling constants). Formylation of compound (*E*)-**6** was then easily accomplished by metalation with *n*-BuLi in THF at –78 °C and subsequent quench with *N*,*N*-DMF. However, ^{1}H-NMR analysis of the crude reaction mixture indicated formation of desired aldehyde **7** together with a side-product in a 10:1 molar ratio, as shown by the presence of two close aldehyde peaks at 9.88 – 9.86 ppm and two sets of ProDOT CH_2 signals at 3.9-4.1 ppm (Figure S1). Fortunately, we determined that the crude 10:1 mixture could still be successfully used for the final Knoevenagel reaction. Indeed, by treatment with cyanoacetic acid in the presence of ammonium acetate / glacial acetic acid, compound **MB25** was predominantly formed, and only a small amount of byproduct was identified by NMR analysis of the crude. Finally, dye **MB25** was obtained in pure form by chromatographic purification and repeated washings with pentane and methanol.

To prepare sensitizer **AD418** (Scheme 2) compound **8** was transformed into intermediate **9**, according to a reported stannylation procedure.[31] The latter was used in a second Pd-catalyzed Stille-Migita coupling with bromide **10**, obtained by treatment of aldehyde **1** with *N*-bromosuccinimide and immediately employed without the need for further purification. In the final step of the synthesis, aldehyde **11** underwent Knoevenagel condensation with cyanoacetic acid in the presence of an AcOH / $AcONH_4$ mixture, to provide dye **AD418** in a satisfactory yield.

The optical properties of the complete series of dyes investigated herein are reported in Figure 3 and Table 1. **DF15**, **MB25** and **AD418** showed a significantly red-shifted absorption compared to **D5** in CH_2Cl_2 solution (Figure 3a), due to the presence of electrondonating alkoxy substituents on the molecular backbone, which enhance the donor-acceptor character of the compounds. This effect was more pronounced for **DF15**, which bears the alkoxy substituents on the donor part of the molecule. On the other hand, **TTZ** dyes display a broader and stronger absorption of visible light, with a maximum at 510-520 nm (Figure 3c). The molar extinction coefficients for **D5**, **DF15**, **MB25** and **AD418** dyes were comprised in the 2.7-3.5 × 10^4 M^{-1} cm^{-1} range, while **TTZ** dyes have much higher molar extinction coefficients, above 8.0 × 10^4 M^{-1} cm^{-1} in THF solution.

Diffuse reflectance spectra (DRS) of the sensitized Pt/TiO_2 photocatalysts used for the H_2 production tests (*see below*) were recorded (Figure 3b, 3d) to investigate the optical properties of the dyes in the solid state. All dyes exhibited a wide absorption band encompassing the visible region in the 400-700 nm range, confirming that they were successfully loaded onto the powder.

Similar to what observed in solution, **DF15** and **MB25** displayed red-shifted spectra relative to **D5**, although in this case the difference was somewhat smaller; **AD418**, on the other hand, gave rise to a DRS spectrum very similar to that obtained with **D5**. Concerning the **TTZ** dye series, no remarkable differences were observed among the curves registered with the different dyes, suggesting that their anchoring mode and adsorption density on Pt/TiO_2 was similar in all cases.

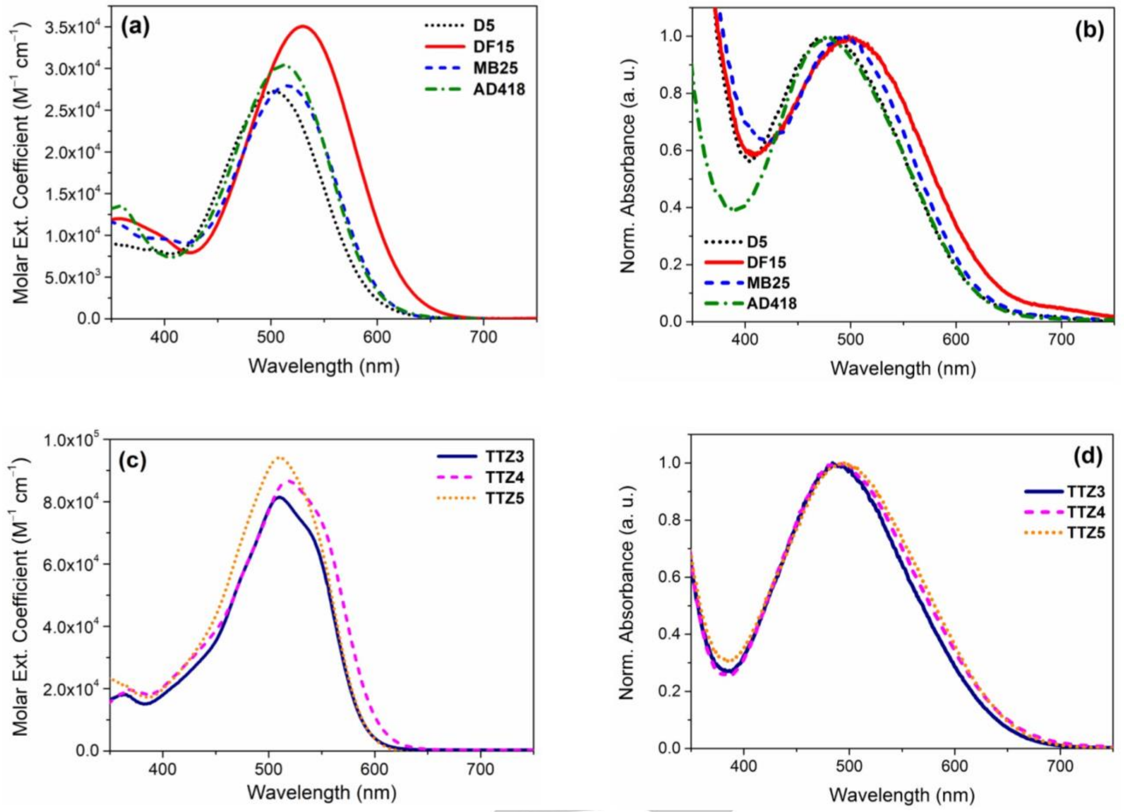

Figure 3. UV-Vis absorption spectra of: (a) compounds **D5**, **DF15**, **MB25** and **AD418** in dichloromethane solution, (c) **TTZ3-5** in THF solution {reproduced from ref. 20}. (b, d) Normalized DRS spectra of the compounds adsorbed on the Pt/TiO_2 catalyst used for hydrogen production tests.

Table 1. Optical and electrochemical properties of the sensitizers employed in this work.

Dye	λ_{max} [nm]	ε [M^{-1} cm^{-1}]	$E_{0\text{-}0}$ [eV][a]	λ_{max} Pt/TiO_2 [nm]	E_{ox} [V][b]	E_{HOMO} [eV][c]	E_{LUMO} [eV][c,d]
D5	501[e]	27300	2.19	478	+1.09[f]	–5.69	–3.50
DF15	530[e,g]	35040[g]	2.07	498	+0.94[g]	–5.54	–3.47
MB25	515[e]	27925	2.14	490	+1.03	–5.63	–3.49
AD418	512[e]	30400	2.16	475	+1.05	–5.65	–3.49
TTZ3	510[h,i]	81400[i]	2.16[i]	484	+1.02[i]	–5.62	–3.46
TTZ4	518[h,i]	86600[i]	2.12[i]	491	+0.77[i]	–5.37	–3.25
TTZ5	510[h,i]	94100[i]	2.16[i]	497	+0.91[i]	–5.51	–3.35

[a] Estimated from the corresponding Tauc plot; [b] Potentials vs. NHE; [c] Values relative to a vacuum, using a potential value of 4.6 ± 0.2 eV for NHE vs. vacuum[34]; [d] Values calculated using the following equation: $E_{LUMO} = E_{HOMO} - E_{0\text{-}0}$; [e] Measured in dichloromethane solution; [f] Value taken from ref. 35; [g] Values taken from ref. 27; [h] Measured in THF solution; [i] Values reproduced from ref. 29.

The optical bandgaps ($E_{0\text{-}0}$) of the dyes were estimated based on the corresponding Tauc plot (Figure S2),[32,33] while their electrochemical properties were determined by means of cyclic voltammetry (Table 1, Figure S3). As expected, the presence of electrondonating groups on the backbone of **DF15**, **MB25** and **AD418** caused a negative shift in the ground-state oxidation potential (E_{ox}) compared to **D5**, in agreement with what observed in the optical measurements. Their LUMO energy, on the other hand, was similar to that of **D5** and in all cases appeared much higher than that of the conduction band of TiO_2 (–4.0 V *vs.* vacuum), thus allowing electron injection from the excited compounds to the semiconductor. Concerning **TTZ4** and **TTZ5,** they clearly showed higher HOMO orbitals compared to the other dyes, which could influence the efficiency of dye regeneration processes, but at the same time presented higher LUMO energies, so that a larger driving force for electron injection in the CB of TiO_2 can be expected for them.

To perform dye-sensitized H_2 photocatalytic production experiments, the investigated dyes were adsorbed over benchmark Pt/TiO_2 nanocomposite catalyst, prepared by photodeposition of Pt on TiO_2 P25, as previously reported.[36] Briefly, the dye was dissolved in THF and was loaded onto the catalyst by mixing its solution with the nanoparticle suspension in EtOH for 12 h in the dark. After filtration, the remaining solution was colorless, indicating quantitative adsorption of the dye. Experiments were first conducted using TEOA as SED at pH = 7.0, under irradiation with visible light (λ > 420 nm, to exclude contribution from TiO_2). After optimization of the experimental conditions,[37] the optimal dye loading was set at 10 µmol g^{-1}. The observed hydrogen production rates with dyes **D5**, **DF15**, **MB25** and **AD418** are shown in Figure 4 and in Table 2.

Independently from the dye employed as sensitizer, the H_2 production rates observed using the sensitized photocatalysts showed an initial increase in the first 1–2 h of illumination, as already observed for similar systems, due to chromatographic effects and to the activation of passivated Pt under irradiation.[36] **D5** and **DF15** showed similar and moderate hydrogen production rates after stabilization (Figure 4), possibly due to a trade-off between the better light-harvesting capability of **DF15**, as demonstrated by its more intense and red-shifted UV-Vis spectrum, and the more positive redox potential of **D5**, which should facilitate its regeneration (for a detailed discussion, see below). In any case, for dye **D5** a rate decrease was observed over time, which was less pronounced in the case of **DF15**. Such phenomenon was evident by looking at the light-to-fuel efficiency (LFE) of the two dyes, which was introduced to quantitatively evaluate the fraction of light energy stored in the form of H_2.[38,39] LFE values after 3 h (LFE_{03}) were almost the same for the two compounds, but after 20 h (LFE_{20}) the value relative to **D5** was almost 25% lower than that of **DF15** (Table 2). Such enhanced stability of **DF15** is consistent with the protecting effect of the long alkyl chains, preventing approach of potential quenchers present in the aqueous environment, in agreement with previous observations.[24] As a result, the overall quantity of produced hydrogen and the TON recorded with **DF15** were slightly superior to those obtained with **D5** (Table 2). **MB25**-sensitized catalysts showed a much higher initial activity, as can be seen by LFE_{03}, but after 4-5 h a sharp decrease in H_2 production was observed, leading to LFE_{20} values similar to those of **D5** and **DF15** at the end of the experiment. Nevertheless, thanks to the excellent performances registered at the beginning of the reaction, TON

Table 2. Photocatalytic performances of the dye/Pt/TiO_2 catalysts in H_2 production with TEOA as SED under irradiation with visible light (λ > 420 nm) for the dyes tested in this study.

Dye	H_2 amount [µmol g^{-1}][a]	TON[b]	LFE_{03}[c]	LFE_{20}[d]
D5	1884	397	0.065%	0.038%
DF15	2371	474	0.066%	0.050%
MB25	2846	569	0.127%	0.041%
AD418	4359	872	0.117%	0.121%
TTZ3	1424	285	0.044%	0.043%
TTZ4	1550	310	0.043%	0.044%
TTZ5	3432	686	0.093%	0.094%

[a] Overall H_2 amount produced after 20 h of irradiation per gram of catalyst; [b] TON = (2 × H_2 total amount after 20h of irradiation)/(dye loading); [c] Light-to-fuel efficiency calculated after 3 h of irradiation; [d] Light-to-fuel efficiency calculated after 20 h of irradiation.

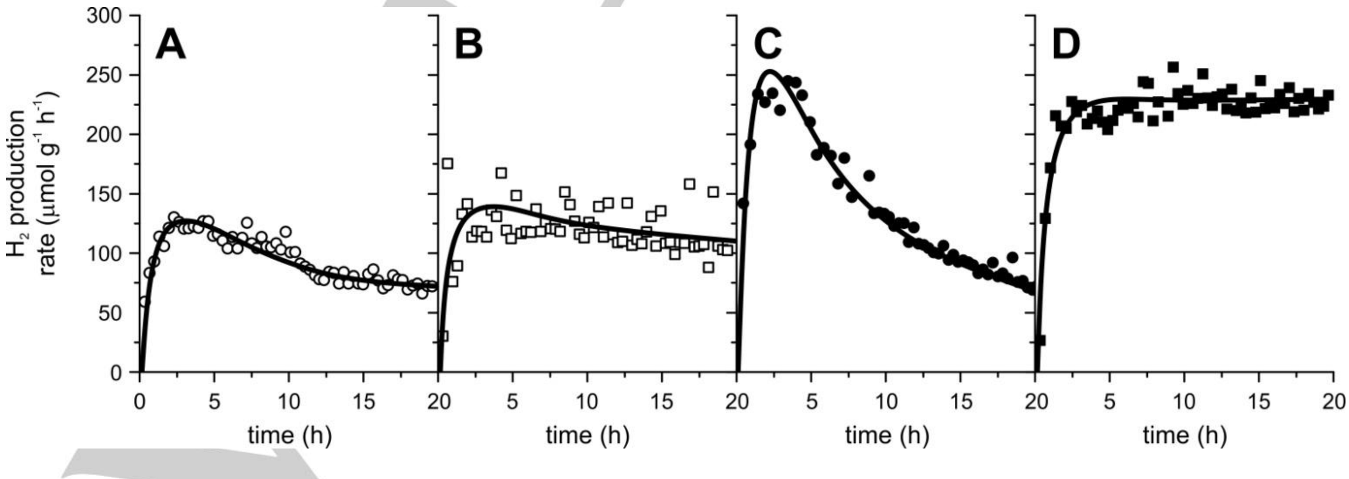

Figure 4. H_2 production from TEOA 10% v/v aqueous solution at pH = 7.0 under irradiation with Vis light (λ > 420 nm) from 0 to 20 h over Pt/TiO_2 catalysts sensitized with: A) **D5**; B) **DF15**; C) **MB25**; D) **AD418**.

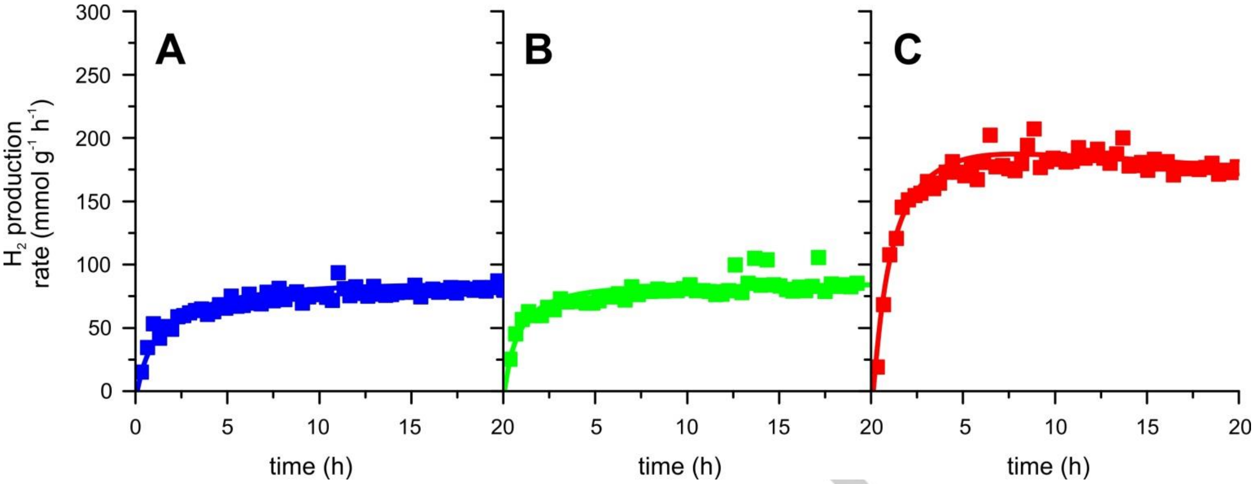

Figure 5. H_2 production from TEOA 10% v/v aqueous solution at pH = 7.0 under irradiation with Vis light (λ > 420 nm) from 0 to 20 h over Pt/TiO_2 catalysts sensitized with: A) **TTZ3**; B) **TTZ4**; C) **TTZ5**.

value for **MB25** was superior to those of the other dyes. The high initial rate of hydrogen production for **MB25** compared to **DF15** was encouraging, as it appeared to confirm our hypothesis that moving the bulky and hydrophobic alkyl chains from the donor to the intermediate part of the molecular scaffold could have a beneficial effect on dye regeneration (by facilitating approach of the SED to the sensitizer) while slowing down undesired recombination events (by better coverage of the TiO_2 surface).

Nevertheless, to better understand the reasons of the observed progressive deactivation of **MB25**, the compounds anchored to TiO_2 at the end of the photocatalysis were characterized with the aim of identifying potential decomposition side-products (See SI for detailed information). UV-Vis and ESI-MS spectroscopy (Figure S4-S6) suggest that a reaction of the unsaturated backbone of **MB25** takes place,[40,41] possibly by protonation followed by nucleophilic addition of water or of a species derived from TEOA (see Figure S7 for a possible pathway involving H_2O). Such process could be favored by the presence of a double bond in the vicinity of the ProDOT unit, which could facilitate protonation thanks to its electrondonating ability.

Such hypothesis is supported by the fact that the photocatalyst obtained by sensitization with **AD418**, an analog of **MB25** in which the double bond was replaced with an extra thiophene moiety (see Figure 2 and Scheme 2), was very active and stable until the end of the experiment, as evident from the hydrogen production rate curve in Figure 4 and the comparison of LFE_{03} and LFE_{20} values (Table 2). Clearly, removing the double bond from the structure of **MB25,** while keeping all other properties as close as possible to the original dye, provided an equally efficient but much more stable sensitizer. As a consequence, the TON value obtained with **AD418** was the highest among the tested dyes.[42]

Thiazolothiazole dyes-sensitized photocatalysts showed intermediate hydrogen production rates compared to the other compounds when TEOA was used as a SED, and were also remarkably stable (Figure 5 and Table 2). **TTZ4** displayed only slightly higher TON values than **TTZ3**, while **TTZ5** showed a much higher H_2 production activity (slightly higher than 3400 μmol g^{-1}, Table 2), relatively close to **AD418**, suggesting that alkyl sulfide substituents on the donor have a beneficial effect in the photocatalytic process. Notably, **TTZ5** was also the best performing sensitizer among **TTZ** dyes in recent DSSC studies carried out by some of us.[28,29]

The dyes employed in the present study have ground-state oxidation potentials ranging from +0.77 V to +1.09 V *vs.* NHE (Table 1), and therefore very close to the reported TEOA redox potential (+0.82 to +1.07 V *vs.* NHE, depending on the conditions).[43,44] Despite that, H_2 production was operative in all cases, clearly demonstrating that dye regeneration was not hampered even in the presence of a seemingly small overpotential. A closer inspection of the data did not reveal any obvious trend linking E_{ox} values with H_2 production rates (Table 1 and 2). Clearly, such observation reflects the fact that H_2 evolution activity depends on the delicate balance of several different factors, among which the properties of the water/dye/TiO_2 interface, influenced by the nature and position of the hydrophobic alkyl chains placed on the sensitizers, play an important role.

In view of the promising results obtained with TEOA, we were interested in evaluating the catalytic performances of the dye sensitized Pt/TiO_2 photocatalysts in combination with a different sacrificial reagent. In particular, ethanol was chosen as SED since it is an environmentally friendly and non-toxic feedstock that can be produced on a large scale from renewable biomass.[16] Ethanol photoreforming has already been investigated for the production of H_2 using several metal/TiO_2 photocatalytic systems,[5,6,9,14] but, to the best of our knowledge, its use as a sacrificial reagent in combination with a dye sensitized photocatalyst has never been reported.

The activity trend emerging from these experiments was very different from that observed in the presence of TEOA. Indeed, when dyes **D5**, **DF15** or **MB25** were used as photosensitizers for the Pt/TiO_2 catalyst in an aqueous EtOH solution, no hydrogen production could be detected. On the contrary, **AD418** and **TTZ3-5** sensitized photocatalysts were active and quite stable in H_2 photocatalytic production, although their TONs were lower than

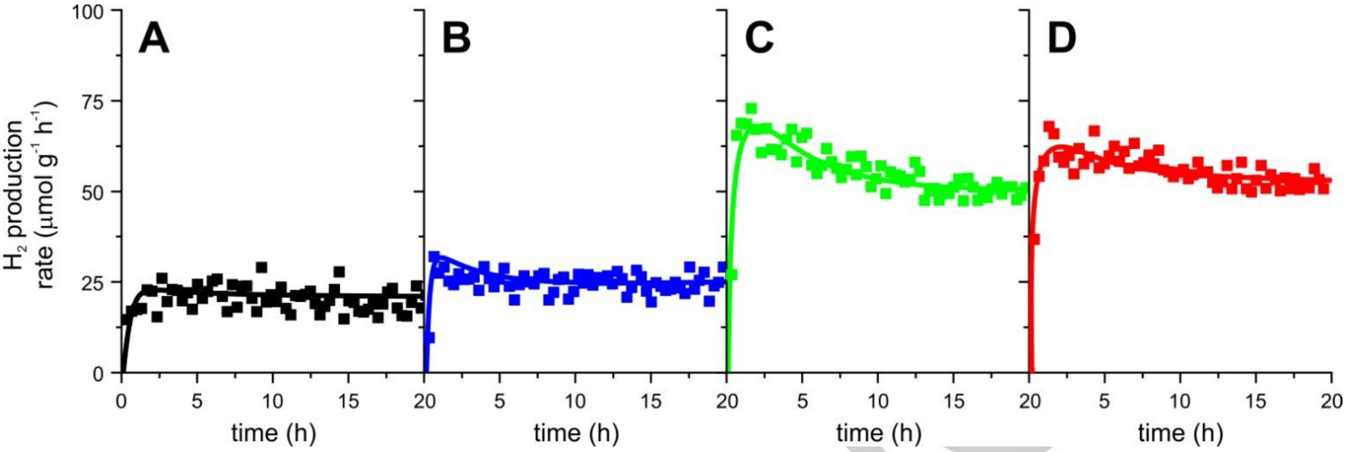

Figure 6. H_2 production rates from EtOH 20% v/v aqueous solution under irradiation with Vis light (λ > 420 nm) from 0 to 20 h over Pt/TiO_2 catalysts sensitized with: A) **AD418**; B) **TTZ3**; C) **TTZ4**; D) **TTZ5**. Please mind the different scale with respect to Figures 4 and 5.

Table 3. Photocatalytic performances of the dye/Pt/TiO_2 catalysts in H_2 production with EtOH as SED under irradiation with visible light (λ > 420 nm) for dyes **AD418** and **TTZ3-5**.

Dye	H_2 amount [µmol g^{-1}][a]	TON[b]	LFE$_{03}$[c]	LFE$_{20}$[d]
AD418	403	81	0.010%	0.009%
TTZ3	493	99	0.014%	0.012%
TTZ4	1102	220	0.033%	0.027%
TTZ5	1105	221	0.033%	0.030%

[a] Overall H_2 amount produced after 20 h of irradiation per gram of catalyst; [b] TON = (2 × H_2 total amount after 20h of irradiation)/(dye loading); [c] Light-to-fuel efficiency calculated after 3 h of irradiation; [d] Light-to-fuel efficiency calculated after 20 h of irradiation.

those observed when TEOA was used as SED, ranging from 80 to 220 (Figure 6, Table 3). More in detail, the catalytic performance obtained with dye **TTZ3** was slightly superior to that registered with dye **AD418**, although the TON improvement was inferior to 20% (Table 3). On the other hand, employment of dyes **TTZ4-5** was more successful, resulting in an increase of more than 2.5 times in hydrogen production rates and TONs. Interestingly, **TTZ4** and **TTZ5** exhibited comparable performance, and were also sufficiently stable over the 20 h of the experiment, as evidenced by the comparison between the light-to-fuel efficiency values calculated at the beginning and at the end of the test. Notably, acetaldehyde was the only product observed in the liquid phase, in stoichiometric amounts compared to H_2 in the gas phase. This is consistent with the oxidation of ethanol into acetaldehyde by the oxidized dye and reduction of protons to H_2 by the photoelectrons injected in the TiO_2 VB, according to reactions (7) and (8). Conversely to un-sensitized photocatalysts, in which photogenerated holes are involved in the process,[3-10] in this case the dyes act as oxidating agents, having suitable potentials for the conversion of ethanol to acetaldehyde (see below).

$$2Dye^{+\cdot} + CH_3CH_2OH \rightarrow 2Dye + CH_3CHO + 2H^{+} \tag{7}$$

$$Pt/TiO_2(e^{-}) + H^{+} \rightarrow Pt/TiO_2/Dye + \frac{1}{2}H_2 \tag{8}$$

With the aim to understand the reason of the different behavior of the various dyes in the presence of EtOH, we re-examined their structural and optoelectronic properties. Compared to dyes **AD418** and **TTZ3**, both compounds **TTZ4**-**5** have electron donating chains placed on the terminal triarylamine unit and display red-shifted absorption spectra when anchored on TiO_2, superior molar extinction coefficients and higher LUMO energies (see the corresponding values in Table 1). The latter observation suggests that a larger driving force for electron injection is especially beneficial to H_2 production efficiency when using EtOH as a SED. We hypothesized that this could be due to a negative shift of TiO_2 CB[45] caused by the adsorption on its surface of negatively-charged ethoxide species formed by the dissociative adsorption of EtOH on TiO_2,[46,47] in turn making electron injection from the LUMO of the excited sensitizers more difficult. To determine if that was the case, we performed selected experiments on **AD418**-sensitized photocatalysts (those showing the largest performance difference when switching from TEOA to EtOH) by running the reaction with TEOA both in the absence and in the presence of EtOH (20% v/v). The results of such experiments suggested that electron injection was not significantly hindered by the alleged ethoxide adsorption, since the H_2 production activity observed using TEOA was only slightly (and positively) affected by EtOH addition, probably due to its capability to act as a “supplementary” SED itself (Figure S8). On the other hand, additional species present in solution (such as, for example, $TEOAH^{+}$ and Cl^{-}, coming from neutralization with aq. HCl, see Experimental Section) could also have an influence on the position of TiO_2 CB, making it difficult to draw a definitive conclusion. However, the resulting effect on hydrogen production rate seemed not very large (Figures 4-6), and therefore CB band shift is likely not the main reason of the lower performances in the presence of the sole EtOH compared to TEOA

Fluorescence lifetime measurements of dyes **D5**, **DF15**, **AD418** and **TTZ5** were then carried out using the time-correlated single photon counting (TCSPC) technique to get further insights in the reason for the different trends observed in the hydrogen production experiments. Samples of the dyes were dissolved in methylene chloride, irradiated with a green led (λ = 499 nm), and the corresponding fluorescence decay curves were recorded (Figure S9). After deconvolution from the instrument response function (IRF), all decay profiles could be fitted with a single exponential function, giving similar excited state lifetimes (τ) comprised in the 1.4 – 2.5 ns range, which did not change significantly when using different solvents and did not seem to correlate with the results of the photocatalytic experiments. Upon absorption of the dyes on TiO_2, a rapid fluorescence quenching was observed in all cases, which confirmed the dyes capability to inject electrons in the semiconductor CB. These results suggest that the different performances of the dyes do not depend on significant differences in the corresponding excited state lifetimes.

Clearly, although thiazolothiazole-bearing dyes were active and stable in H_2 photocatalytic production, ethanol appeared a much less efficient SED compared to TEOA, despite being a thermodynamically competent reducing agent. Indeed, its one-electron oxidation potential in aqueous solution has been measured several times by means of cyclic voltammetry in a range of different conditions,[48-51] and was found to shift from approx. 0.0 V *vs*. NHE in strongly basic medium[52] to approx. +0.9 V *vs*. NHE in strongly acidic solution,[53] values generally compatible with the ground-state oxidation potentials of all dyes used in this study (+0.77 - +1.09 V *vs.* NHE, Table 1). Thus, the observed results suggest that the efficiency of the selected SED is not only dictated by its thermodynamic ability to reduce the oxidized photosensitizer, but also by the kinetic barrier for the electron transfer process. In this regard, it has been already observed that TEOA is a more efficient hole-scavenger than methanol or ethanol in photocatalytic H_2 generation processes using inorganic[54,55] or carbon-based catalysts,[56] and this difference has been ascribed to the fact that TEOA can use the lone pair of nitrogen for the first electron transfer,[57] in agreement with earlier reports indicating that only the deprotonated form of the amine is an active reducing agent.[43] Based on relevant literature references on TEOA[58] and alcohol photoreforming,[3,5,10,14] a mechanistic proposal for the two different regeneration processes is presented in Figure S10, bearing in mind that in this instance no photogenerated holes are present on TiO_2 due to the filtering of simulated solar light.

In our case, the slower dye regeneration when ethanol is used could compete with charge recombination between injected electrons and the oxidized dye, hampering the H_2 production process. In this hypothesis, the excellent spectroscopic properties and the large driving force for electron injection displayed by dyes **TTZ4-5** should enhance the efficiency of the elementary light-harvesting and charge injection steps, increasing the electron density on TiO_2 and ultimately improving hydrogen production rates.

Conclusions

In this work, we presented the results obtained in the photocatalytic hydrogen production using dye-sensitized Pt/TiO_2 catalysts in combination with two different sacrificial reagents (TEOA and EtOH). All sensitizers were metal-free organic compounds characterized by a D-π-A structure, and some of them (compounds **TTZ3-5**) featured a thiazolo[5,4-*d*]thiazole internal unit introduced to modulate their light-absorption and electronic properties. The sensitizers were endowed with hydrophobic alkyl chains on different parts of their molecular scaffold, whose position and number was systematically altered to evaluate their influence on catalytic performances.

When employing TEOA as SED, the best result was obtained with sensitizer **AD418**, carrying a propylenedioxythiophene (ProDOT) moiety on the intermediate part of the structure. Comparison of its performance with that yielded by compound **DF15** (bearing linear alkoxy substituents on its donor group) supported the hypothesis that placing alkyl chains on the conjugated molecular scaffold rather than on the donor could have a beneficial effect on dye regeneration while slowing down undesired recombination events.

Thiazolothiazole-bearing dyes, in particular **TTZ4** and **TTZ5** provided the best results when using EtOH as SED. Such behavior is especially interesting as use of EtOH as a sacrificial reagent in combination with a dye sensitized photocatalyst had never been described so far. Analysis of the molecular structure as well as their electronic properties of the dyes suggested that in this case dye regeneration is slower, so charge recombination between injected electrons in TiO_2 and the oxidized dye can hinder the photocatalytic process. Thus, a stronger light harvesting capability coupled with a larger driving force for electron injection can help increasing the electron density on TiO_2, thereby enhancing hydrogen production rates.

This study indicates that the molecular design of sensitizers should be carefully adjusted depending on the particular SED (and set of conditions) used in the experiments in order to yield the best results in hydrogen production experiments. Finely tuned sensitizers may lead to a breakthrough in dye-sensitized photocatalytic H_2 production sustainability, extending the range of efficient SEDs to alcohols and possibly other biomass-derived feedstocks.

Experimental Section

General Experimental Remarks. All air-sensitive reactions were performed under inert atmosphere in a flame- or oven-dried apparatus using Schlenk techniques. Solvents used in metal-catalyzed reactions were degassed by means of the "*freeze-pump-thaw*" method. Tetrahydrofuran (THF) was distilled over metallic sodium with benzophenone as an indicator, methanol was distilled from metallic magnesium in the presence of iodine (cat.), CH_2Cl_2 was distilled over CaH_2. Toluene was dried on a resin exchange Solvent Purification System (*MBraun*). 3,3-Dipentyl-3,4-dihydro-*2H*-thieno[3,4-*b*][1,4]dioxepine-6-carbaldehyde (**1**),[30] *N*,*N*-diphenyl-4-(5-(tributylstannyl)thiophen-2-yl)aniline (**9**),[31] and dyes **DF15**[27] and **TTZ3-5**[28,29] were prepared as previously reported. 4-(diphenylamino)-benzaldehyde (**5**) and all other chemicals employed were commercially available and used as received. Thin-layer chromatography was carried out on aluminum-supported plates

10.1002/cssc.201701707

coated with a fluorescent indicator; detection was carried out using UV light (λ = 254 and 365 nm) and permanganate or molybdophosphoric acid solutions followed by heating. Flash column chromatography was performed using Merck Kieselgel 60 (300-400 mesh) as the stationary phase. ^{1}H-NMR spectra were recorded at 300 or 400 MHz, ^{13}C-NMR spectra were recorded at 75.5 or 100.6 MHz, respectively, and ^{31}P-NMR spectra were recorded at 121 MHz. Chemical shifts were referenced to the residual solvent peak ($CDCl_3$, δ 7.26 ppm for ^{1}H-NMR, δ 77.16 ppm for ^{13}C-NMR; THF-*d8,* δ 1.72 and 3.58 ppm for ^{1}H-NMR, δ 25.31 and 67.21 ppm for ^{13}C-NMR). FT-IR spectra were recorded in the range 4000-400 cm^{-1} with a 2 cm^{-1} resolution. ESI-MS spectra were obtained by direct injection of the sample and are reported in the form *m/z* (intensity relative to base = 100).

(3,3-dipentyl-3,4-dihydro-*2H*-thieno[3,4-*b*][1,4]dioxepin-6-yl)methanol (2). 3,3-dipentyl-3,4-dihydro-*2H*-thieno[3,4-*b*][1,4]dioxepine-6-carbaldehyde (**1**, 1.02 g, 3.15 mmol, 1.0 eq) was dissolved in CH_2Cl_2 (15 mL) and methanol (20 mL), then, after cooling to 0 °C, sodium borohydride (0.202 g, 5.34 mmol, 1.7 eq.) was added into the reaction vessel. The resulting mixture was stirred at 0 °C for 30 minutes, then at room temperature for other 30 minutes. A saturated aqueous solution of NH_4Cl (45 mL) was added into the flask and the mixture was stirred until hydrogen production ceased, then the two phases were separated. The aqueous phase was extracted with CH_2Cl_2 (2 × 15 mL), then the combined organic phases were washed with brine and dried with Na_2SO_4. After filtration, removal of the solvent afforded alcohol **2** (1.01 g, 3.09 mmol, 98% yield) as an orange oil which was used for the next step without further purification. ^{1}H–NMR (300 MHz, $CDCl_3$): δ = 6.36 (s, 1H), 4.61 (s, 2H), 3.84 (s, 2H), 3.82 (s, 2H), 2.41 (bs, 1H), 1.26–1.34 (m, 16H), 0.89 (t, *J* = 7.0 Hz, 6H) ppm. ^{13}C–NMR (75 MHz, $CDCl_3$): δ = 149.5, 146.8, 121.2, 103.2, 77.2, 76.7, 56.7, 43.9, 32.7, 31.8, 22.6, 22.5, 14.1 ppm. IR (KBr): $\tilde{\nu}$ = 3410, 3112, 2930, 2861, 1459, 1412, 1376, 1206, 1164, 1016 cm^{-1}. ESI–MS: *m/z* = 349 [M+Na]$^{+}$, 309 [M–OH]$^{+}$.

Diethyl ((3,3-dipentyl-3,4-dihydro-*2H*-thieno[3,4-*b*][1,4]dioxepin-6-yl)methyl)phosphonate (4). Alcohol **2** (1.39 g, 4.25 mmol, 1.0 eq.) was dissolved in THF (30 mL), then the solution was cooled to –5 °C and PBr_3 (1.17 g, 4.33 mmol, 0.41 mL, 3.0 eq.) was added into the reaction vessel. The resulting dark mixture was stirred at 0 °C for 30 minutes, then triethyl phosphite (2.12 g, 12.8 mmol, 2.17 mL, 3.0 eq.) was added dropwise at room temperature. The resulting mixture was stirred at reflux for 7 h and then at 60 °C for 10 h. After cooling to room temperature, the solvent was removed under vacuum. Purification by flash column chromatography (SiO_2, petroleum ether/AcOEt from 3:1 to 1:1) afforded desired product **4** (1.56 g, 3.49 mmol, 82% yield) as a yellow oil. ^{1}H–NMR (300 MHz, $CDCl_3$): δ = 6.31 (d, *J* = 2.7 Hz, 1H), 4.03–4.13 (m, 4H), 3.82 (s, 2H), 3.80 (s, 2H), 3.20 (d, *J* = 20.3, 2H), 1.33–1.25 (m, 22H), 0.88 (t, *J* = 7.0 Hz, 6H) ppm. ^{13}C–NMR (75 MHz, $CDCl_3$): δ = 149.3 (d, *J* = 3.6 Hz), 147.4 (d, *J* = 9.7 Hz), 111.5 (d, *J* = 11.3 Hz), 102.5 (d, *J* = 4.2 Hz), 77.9, 77.8, 62.4 (d, *J* = 6.5 Hz), 44.0, 32.8 (×2), 31.7 (×2), 24.6 (d, *J* = 144.3 Hz), 22.7 (×2), 22.6 (×2), 16.5 (d, *J* = 6.0 Hz), 14.2 (×2) ppm. ^{31}P–NMR (121 MHz, $CDCl_3$): δ = 24.5 (s) ppm. IR (KBr): $\tilde{\nu}$ = 3112, 2930, 1724, 1648, 1497, 1377, 1258, 1029 cm^{-1}. ESI–MS: *m/z* = 915 [2M+Na]$^{+}$, 447 [M+H]$^{+}$.

(*E*)-4-(2-(3,3-dipentyl-3,4-dihydro-*2H*-thieno[3,4-*b*][1,4]dioxepin-6-yl)vinyl)-*N*,*N*-diphenylaniline (6). 4-(diphenylamino)-benzaldehyde (**5**, 53 mg, 0.19 mmol, 1.0 eq.) was dissolved in THF (0.3 mL), then a solution of phosphonate **4** (100 mg, 0.22 mmol, 1.2 eq.) in THF (1.0 mL) was added to the reaction vessel. After cooling to 0 °C, NaHMDS (70 mg, 0.38 mmol, 2.0 eq.) was added. The reaction mixture was stirred at 0 °C for 15 minutes, then at room temperature for other 15 minutes and, finally, at reflux temperature for 16 h. After cooling to room temperature, water (4 mL) was added and the resulting mixture was concentrated under vacuum. After dilution with ethyl acetate (5 mL), the two phases were separated. The aqueous phase was washed with fresh ethyl acetate (3 × 10 mL), then the combined organic phases were washed with brine (20 mL) and dried with Na_2SO_4. After filtration and removal of the solvent under vacuum, the reaction crude was purified by flash column chromatography (SiO_2, petroleum ether/AcOEt 30:1). Desired product **6** (83 mg, 0.15 mmol, 76% yield) was isolated as a dense yellow oil. ^{1}H–NMR (300 MHz, $CDCl_3$): δ = 7.30–7.37 (m, 2H), 7.21–7.30 (m, 4H), 7.07–7.15 (m, 5H), 6.98–7.06 (m, 4H), 6.73 (d, *J* = 16.2 Hz, 1H), 6.28 (s, 1H), 3.92 (s, 2H), 3.86 (s, 2H), 1.26–1.39 (m, 16H), 0.91 (t, *J* = 7.0 Hz, 6H) ppm. ^{13}C–NMR (75 MHz, $CDCl_3$): δ = 150.1, 147.7, 147.1, 146.7, 131.8, 129.4, 127.2, 125.6, 124.5, 123.8, 123.1, 122.0, 117.4, 101.8, 77.9, 77.7, 43.9, 32.8 (×2), 32.0 (×2), 22.7 (×2), 22.6 (×2), 14.2 (×2) ppm. IR (KBr): $\tilde{\nu}$ = 3026, 2927, 1591, 1483, 1375, 1277, 1030 cm^{-1}. ESI–MS: *m/z* = 565 [M]$^{+}$.

(*E*)-8-(4-(diphenylamino)styryl)-3,3-dipentyl-3,4-dihydro-*2H*-thieno[3,4-*b*][1,4]dioxepine-6-carbaldehyde (7). Compound **6** (0.85 g, 1.53 mmol, 1.0 eq.) was dissolved in THF (15 mL), then, after cooling to –78 °C, *n*-BuLi (1.6 M solution in pentane, 1.40 mL, 2.25 mmol, 1.5 eq) was added in the reaction vessel. After one hour under stirring at – 78 °C, *N,N*-DMF (0.22 g, 3.00 mmol, 0.23 mL, 2.0 eq.) was added, then the reaction mixture was slowly warmed to room temperature and stirred for 16 h. After this time, a saturated aqueous solution of NH_4Cl (12 mL) was added, then THF was evaporated under vacuum and the aqueous phase was extracted with ethyl acetate (3 × 30 mL). The combined organic phases were washed with brine (2 × 70 mL) and dried with Na_2SO_4. After filtration and removal of the solvent under vacuum, a dense orange oil corresponding to a 10:1 mixture of aldehyde **7** and an unidentified side product (0.84 g, 90% approx. yield of aldehyde **7**) was obtained and used as such for the following reaction. Characterization data for aldehyde **7**: ^{1}H–NMR (300 MHz, $CDCl_3$): δ = 9.88 (s, 1H), 6.95–7.37 (m, 16H), 4.07 (s, 2H), 3.98 (s, 2H), 1.25–1.42 (m, 16H), 0.91 (t, *J* = 6.8 Hz, 6H) ppm. ^{13}C–NMR (75 MHz, $CDCl_3$): δ = 180.6, 156.7, 148.3, 147.4, 145.8, 132.8, 130.7, 130.1, 129.5, 128.0, 125.0, 123.6, 123.0, 118.2, 116.0, 78.2, 78.0, 43.9, 32.7 (×2), 32.2 (×2), 22.7 (×4), 14.2 (×2) ppm. IR (KBr): $\tilde{\nu}$ = 2924, 1642, 1589, 1485, 1424, 1278, 1049 cm^{-1}. ESI–MS: *m/z* = 608 [M+Me]$^{+}$ (*peak derived from the formation of the emiacetal of aldehyde* ***7*** *with MeOH)*.

(*E*)-2-cyano-3-(8-((*E*)-4-(diphenylamino)styryl)-3,3-dipentyl-3,4-dihydro-*2H*-thieno[3,4-*b*][1,4]dioxepin-6-yl)acrylic acid (MB25). Aldehyde **7** (0.48 g, 0.82 mmol, 1.0 eq.), as obtained in the previous step, was dissolved in toluene (45 mL), then cyanoacetic acid (0.69 g, 8.15 mmol, 10 eq.), ammonium acetate (0.25 g, 3.28 mmol, 4.0 eq.) and acetic acid (65 mL) were added to the reaction vessel. The reaction mixture was heated under stirring at 120° C for 4 h, then cooled to room temperature and diluted with AcOEt (200 mL). The organic phase was washed with aq. NH_4Cl 1M (230 mL + 4 × 70 mL) and brine (150 mL), then dried with Na_2SO_4. After filtration and removal of the solvent under vacuum, the reaction crude was purified by flash column chromatography (SiO_2, CH_2Cl_2, then CH_2Cl_2/AcOH 98:2). Desired product **MB25** (0.35 g, 0.53 mmol, 65% yield) was isolated as dark red solid. ^{1}H–NMR (300 MHz, $CDCl_3$): δ = 8.41 (s, 1H), 7.33–7.40 (m, 2H), 7.24–7.32 (m, 4H), 7.04–7.16 (m, 8H), 6.97–7.04 (m, 2H), 4.10 (s, 2H), 3.98 (s, 2H), 1.31–1.39 (m, 16H), 0.91 (t, *J* = 6.9 Hz, 6H) ppm. ^{13}C–NMR (75 MHz, $CDCl_3$): δ = 169.1, 156.8, 148.7, 147.2, 145.7, 143.5, 135.3, 132.5, 129.7, 129.5, 128.3, 125.2, 123.8, 122.5, 116.8, 115.3, 113.2, 91.5, 78.3, 77.4, 43.7, 32.7 (×2), 32.2 (×2), 22.7 (×4), 14.2 (×2) ppm. IR (KBr): $\tilde{\nu}$ = 3423, 2930, 2857, 2213, 1681, 1564, 1480, 1242, 1049 cm^{-1}. ESI-MS: *m/z* = 661 [M+1]$^{+}$.

8-(5-(4-(diphenylamino)phenyl)thiophen-2-yl)-3,3-dipentyl-3,4-dihydro-*2H*-thieno[3,4-*b*][1,4]dioxepine-6-carbaldehyde (11). 3,3-dipentyl-3,4-dihydro-*2H*-thieno[3,4-*b*][1,4]dioxepine-6-carbaldehyde (**1**, 0.35 g, 1.08 mmol, 1.0 eq) was dissolved in chloroform (8 mL) and acetic acid (4 mL), then *N*-bromosuccinimide (0.21 g, 1.19 mmol, 1.1 eq.) was added to the reaction vessel. The reaction mixture was stirred at room temperature for 1.5 h, then, after dilution with chloroform (30 mL), the organic phase was washed with a saturated aqueous solution of $NaHCO_3$ (40 mL) and brine (40 mL) and dried with Na_2SO_4. After filtration, the solvent was removed under vacuum. The reaction crude was dissolved in *N*,*N*-DMF (10 mL), then *N*,*N*-diphenyl-4-(5-(tributylstannyl)thiophen-2-yl)aniline (**9**, 0.727 g, 1.18 mmol, 1.1 eq.) and $Pd(PPh_3)_2Cl_2$ (0.038 g, 0.054 mmol, 5.0 mol%) were added to the reaction vessel. The mixture was stirred at 90 °C for 2 h, then, after cooling, to room temperature, filtered over Celite®. The filtrate was diluted with ethyl acetate (50 mL) and the organic phase was washed with water (4 × 50 mL) and brine (2 × 50 mL). After dehydration with Na_2SO_4, filtration and removal of the solvent under vacuum, flash column chromatography (SiO_2, petroleum ether/ CH_2Cl_2 gradient from 3:1 to 1:1) afforded desired product **11** (0.47 g, 0.72 mmol, 67% yield) as a dark red solid. ^{1}H–NMR (400 MHz, $CDCl_3$): δ = 9.90 (s, 1H), 7.48 (d, *J* = 8.6 Hz, 2H), 7.36 (d, *J* = 3.9 Hz, 1H), 7.24–7.30 (m, 4H), 7.16 (d, *J* = 3.9 Hz, 1H), 7.12 (d, *J* = 7.7 Hz, 4H), 7.02–7.08 (m, 4H), 4.11 (s, 2H), 4.06 (s, 2H), 1.42–1.49 (m, 4H), 1.25–1.38 (m, 12H), 0.92 (t, *J* = 6.1 Hz, 6H). ^{13}C–NMR (100 MHz, $CDCl_3$): δ = 180.5, 156.7, 147.9, 147.4, 146.2, 144.1, 132.2, 129.5, 127.7, 126.9, 126.7, 124.8, 123.4, 122.4, 117.7, 78.3, 78.2, 44.0, 32.7, 32.2, 22.7, 14.2. (*Two carbon signals are missing, likely covered by other signals*). ESI-MS: *m/z* = 649 [M]$^+$; 695 [M$^+$, dimethylacetal of aldehyde **11**]$^+$. IR (KBr): 3070, 2956, 2928, 2857, 1647, 1593, 1485, 1426, 1281, 1051 cm^{-1}.

(*E*)-2-cyano-3-(8-(5-(4-(diphenylamino)phenyl)thiophen-2-yl)-3,3-dipentyl-3,4-dihydro-2*H*-thieno[3,4-*b*][1,4]dioxepin-6-yl)acrylic acid (AD418). Aldehyde **11** (0.075 g, 0.115 mmol, 1.0 eq) was dissolved in toluene (2 mL), then a solution of cyanoacetic acid (0.098 g, 1.15 mmol, 10 eq.) and ammonium acetate (0.035 g, 0.46 mmol, 4.0 eq.) in acetic acid (2 mL) was added in the reaction vessel. The mixture was stirred at 100 °C for 4 h, then, after cooling to room temperature, the solvent was removed and replaced with DCM (30 mL). The organic phase was washed with aq. HCl 0.03 M (30 mL) and brine (30 mL), and dried with Na_2SO_4. After filtration and removal of the solvent, washings of the crude with small portions of pentane and methanol afforded the desired product **AD418** (0.076 g, 0.106 mmol, 92% yield) as a dark purple solid. ^{1}H–NMR (400 MHz, THF-*d8*): δ = 8.33 (s, 1H), 7.55 (d, *J* = 8.2 Hz, 2H), 7.48 (d, *J* = 3.3 Hz, 1H), 7.32 (d, *J* = 3.5 Hz, 1H), 7.24–7.28 (m, 4H), 7.09 (d, *J* = 7.8 Hz, 4H), 7.00–7.06 (m, 4H), 4.17 (s, 2H), 4.12 (s, 2H), 1.46–1.52 (m, 4H), 1.25–1.42 (m, 12H), 0.92 (t, *J* = 5.9 Hz, 6H). ^{13}C–NMR (100 MHz, THF-*d8*): δ = 164.4, 156.3, 148.7, 148.2, 147.1, 145.0, 141.3, 132.7, 130.0, 128.6, 127.8, 127.2, 127.0, 125.3, 124.1, 123.9, 123.4, 116.9, 113.2, 95.8, 79.0, 78.8, 44.4, 33.4, 32.7, 23.23, 23.17, 14.2. ESI-MS: *m/z* = 716.48 [M]$^+$. IR (KBr): 3447, 3061, 2928, 2860, 2214, 1654, 1576, 1542, 1419, 1251 cm^{-1}. HRMS (ESI) for $C_{43}H_{44}O_4N_2S_2$ [M$^+$]: calcd 716.2737, found 716.2741.

Optical and electrochemical measurements. UV-Vis absorption spectra were recorded on diluted solutions of the compounds (approx. 10^{-5} M in the solvents specified in the text). DRS spectra were recorded on sensitized Pt/TiO_2 catalyst powders in the reflectance mode using an integrating sphere (with Ba_2SO_4 as a reference standard), and were converted to the corresponding absorption spectra using the Kubelka-Munk equation. Cyclic voltammetry experiments were conducted in dichloromethane solution employing a three-electrode cell having a glassy carbon working electrode, a platinum counter-electrode and an aqueous Ag/AgCl (sat. KCl) reference electrode. The supporting electrolyte was electrochemical-grade $[N(Bu)_4]PF_6$. Under these experimental conditions, the one-electron oxidation of ferrocene occurs at $E^{\circ\prime}$ = 0.62 V.

The technique used for the measurement of the fluorophores lifetime is the Time Correlated Single Photon Counting (TCSPC).[59] The apparatus consisted of a PDL 808 “Sepia” laser driver system, a TimeHarp 200 PCI acquisition board, a PMA182-P-M photomultiplier (PM) detector and a PLS 500 collimated LED source, all from PicoQuant (Germany). The chosen LED source had peak emission wavelength at 499 nm, average maximum power of 33 μW, peak power of 947 μW, pulse energy of 0.83 pJ, spectral width of 50 nm (FWHM) and time pulse duration of 947 ps (FWHM). The acquisition system allowed to acquire 4096 time channels with a minimum time resolution of 34 ps. The sample was directly illuminated by the collimated LED light (excitation light). The fluorescence signal was collected at an angle of 90 degrees with respect to the excitation direction by means of a 200 μm core diameter multimode fiber coupled with a 1 mm diameter GRIN lens, so that only collimated photons could be collected. The other end of the fiber was coupled with a 1 mm GRIN lens and then faced to the PM detector. The instrument response function (IRF) was collected using an aqueous suspension of polystyrene latex beads. Data were analyzed by means of Picoquant FluoFit 4.4 fluorescence decay data analysis software.

Preparation of Pt/TiO_2 nanopowder. Pt was photodeposited on TiO_2 Degussa P25 following a previously reported procedure.[18a,60] Briefly, 2 g of TiO_2 Degussa P25 were suspended in 400 mL $Pt(NO_3)_2$ aqueous solution (EtOH 50 % v/v), in order to reach a final Pt loading of 1.0 wt%. After stirring for 1 h in the dark, the suspension was irradiated with a 450 W medium pressure Hg lamp for 4 h. Nanopowders were recovered through centrifugation, washed with EtOH 3 times, and dried under vacuum at 50 °C overnight.

Dyes adsorption on Pt/TiO_2. 200 mg of Pt/TiO_2 nanopowder was suspended in 20 mL of dye solution (0.1 mM in ethanol) for 24 h in the dark. Then, the nanopowder was separated through centrifugation, washed twice with ethanol, and dried under vacuum at room temperature overnight. After staining, the concentration of the dyes in the solution was measured by UV-vis spectroscopy. More than 95% of the dye was adsorbed on the Pt/TiO_2 material in all cases.

Hydrogen production through photoreforming. The dye-sensitized Pt/TiO_2 nanomaterials have been tested for H_2 production using TEOA or EtOH as sacrificial electron donors, following or slightly modifying a previously described procedure.[36] 60 mg of the dye-sensitized Pt/TiO_2 catalyst was suspended into 60 mL of either 10 % v/v aqueous solution of TEOA previously neutralized with HCl, or 20 % v/v aqueous solution of EtOH. After purging with Ar (15 mL min^{-1}) for 30 min, the suspension was irradiated using a 150 W Xe lamp with a cut-off filter at 420 nm. Irradiance was ~ 6 x 10^{-3} W m^{-2} in the UV-A range and ~ 1080 W m^{-2} in the visible and near-IR range (400 – 1000 nm). The concentration of H_2 in gas stream coming from the reactor has been quantified using a Agilent 7890 gaschromatograph equipped with a TCD detector, connected to a Carboxen 1010 column (Supelco, 30 m x 0.53 mm ID, 30 μm film) using Ar as carrier. Blank experiments on Pt/TiO_2 in the absence of dyes showed no H_2 evolution under any of the experimental conditions used in this work. The performances of the sensitized photocatalysts have been reported in terms of H_2 production rate and overall H_2 productivity. Turn-Over Numbers (TON) were calculated from the total amount of H_2 produced in 20h of irradiation as:

$$TON = \frac{2\ x\ overall\ H_2\ amount\ (\mu mol\ g^{-1})}{2\ x\ dye\ loading\ (\mu mol\ g^{-1})}$$

Light-to-Fuel Efficiency (LFE) was calculated as:

$$LFE = \frac{F_{H_2}\ \Delta H^0{}_{H_2}}{S\ A_{irr}}$$

where F_{H2} is the flow of H_2 produced (expressed in mol s^{-1}), $\Delta H^0{}_{H2}$ is the enthalpy associated with H_2 combustion (285.8 kJ mol^{-1}), S is the total incident light irradiance, as measured by adequate radiometers in 400 – 1000 nm range (expressed in W cm^{-2}) and A_{irr} is the irradiated area (expressed in cm^2). UV-vis spectra of the aqueous solutions recovered at the end of the photocatalytic runs highlighted that no desorption of the dyes took place during the experiments.

Acknowledgements

M.M., T.M., and P.F. acknowledge financial support from University of Trieste through the FRA2015 project. All the other authors thank the Cassa di Risparmio di Firenze Foundation for funding through the ENERGYLAB project.

Keywords: Photocatalytic hydrogen production • Photosensitizers • Donor-acceptor dyes • Heterocyclic chemistry • Ethanol photoreforming.

[1] R. C. Armstrong, C. Wolfram, K. P. de Jong, R. Gross, N. S. Lewis, B. Boardman, A. J. Ragauskas, K. Ehrhardt-Martinez, G. Crabtree, M. V. Ramana, *Nat. Energy* **2016**, *1*, 15020.

[2] J. Schneider, M. Matsuoka, M. Takeuchi, J. Zhang, Y. Horiuchi, M. Anpo, D. W. Bahnemann, *Chem. Rev.* **2014**, *114*, 9919-9986.

[3] X. Fu, J. Long, X. Wang, D. Y. C. Leung, Z. Ding, L. Wu, Z. Zhang, Z. Li, X. Fu, *Int. J. Hydrogen En.* **2008**, *33*, 6484-6491.

[4] Q. Gu, J. Long, Y. Zhou, R. Yuan, H. Lin, X. Wang, *J. Catal.* **2012**, *289*, 88-99.

[5] Q. Gu, J. Long, L. Fan, L. Chen, L. Zhao, H. Lin, X. Wang, *J. Catal.* **2013**, *303*, 141-155.

[6] A. V. Puga, A. Forneli, H. García, A. Corma, *Adv. Funct. Mater.* **2014**, *24*, 241-248.

[7] J. Long, H. Chang, Q. Gu, J. Xu, L. Fan, S. Wang, Y. Zhou, W. Wei, L. Huang, X. Wang, P. Liu, W. Huang, *Energy Environ. Sci.* **2014**, *7*, 973-977.

[8] L. Fan, J. Long, Q. Gu, H. Huang, H. Lin, X. Wang, *J. Catal.* **2014**, *320*, 147-159.

[9] Q. Gu, J. Long, H. Zhuang, C. Zhang, Y. Zhou, X. Wang, *Phys. Chem. Chem. Phys.* **2014**, *16*, 12521-12534.

[10] R. Jaswal, R. Shende, W. Nan, A. Shende, *Int. J. Hydrogen. En.* **2017**, *42*, 2839-2848.

[11] A. Hagfeldt, G. Boschloo, L. Sun, L. Kloo, H. Pettersson, *Chem. Rev.* **2010**, *110*, 6595-6663.

[12] B. Cecconi, N. Manfredi, T. Montini, P. Fornasiero, A. Abbotto, *Eur. J. Org. Chem.* **2016** 5194-5215.

[13] X. Zhang, T. Peng, S. Song, *J. Mater. Chem. A* **2016**, *4*, 2365-2402.

[14] K. C. Christoforidis, P. Fornasiero, *ChemCatChem* **2017**, 9, 1523-1544.

[15] (a) X. Li, S. Cui, D. Wang, Y. Zhou, H. Zhou, Y. Hu, J.-g. Liu, Y. Long, W. Wu, J. Hua, H. Tian, *ChemSusChem* **2014**, *7*, 2879-2888; (b) S. Balasubramanian, P. Wang, R. D. Schaller, T. Rajh, E. A. Rozhkova, *Nano Lett.* **2013**, *13*, 3365-3371.

[16] S. Zinoviev, F. Müller-Langer, P. Das, N. Bertero, P. Fornasiero, M. Kaltschmitt, G. Centi, S. Miertus, *ChemSusChem.* **2010**, *3*, 1106–1133.

[17] X. Zhang, B. Peng, S. Zhang, T. Peng, *ACS Sust. Chem. Eng.* **2015**, *3*, 1501–1509.

[18] (a) S.-H. Lee, Y. Park, K.-R. Wee, H.-J. Son, D. W. Cho, C. Pac, W. Choi, S. O. Kang, *Org. Lett.* **2010**, *12*, 460-463; (b) W.-S. Han, K.-R. Wee, H.-Y. Kim, C. Pac, Y. Nabetani, D. Yamamoto, T. Shimada, H. Inoue, H. Choi, K. Cho, S. O. Kang, *Chem. Eur. J.* **2012**, *18*, 15368-15381.

[19] N. Manfredi, B. Cecconi, V. Calabrese, A. Minotti, F. Peri, R. Ruffo, M. Monai, I. Romero-Ocaña, T. Montini, P. Fornasiero, A. Abbotto, *Chem. Commun.* **2016**, *52*, 6977-6980.

[20] M. Watanabe, H. Hagiwara, A. Iribe, Y. Ogata, K. Shiomi, A. Staykov, S. Ida, K. Tanaka, T. Ishihara, *J. Mater. Chem. A* **2014**, *2*, 12952-12961.

[21] A. Tiwari, U. Pal, *Int. J. Hydrogen En.* **2015**, *40*, 9069-9080.

[22] A. Kumari, I. Mondal, U. Pal, *New J. Chem.,* **2015**, *39*, 713-720.

[23] K. Narayanaswamy, A. Tiwari, I. Mondal, U. Pal, S. Niveditha, K. Bhanuprakash, S. P. Singh, *Phys. Chem. Chem. Phys.* **2015**, *17*, 13710-13718.

[24] J. Lee, J. Kwak, K. C. Ko, J. H. Park, J. H. Ko, N. Park, E. Kim, D. H. Ryu, T. K. Ahn, J. Y. Lee, S. U. Son, *Chem. Commun.* **2012**, *48*, 11431-11433.

[25] A. Tiwari, I. Mondal, U. Pal, *RSC Adv.* **2015**, *5*, 31415-31421.

[26] (a) D. P. Hagberg, T. Edvinsson, T. Marinado, G. Boschloo, A. Hagfeldt, L. Sun, *Chem. Commun.* **2006**, 2245-2247; (b) D. P. Hagberg, T. Marinado, K. M. Karlsson, K. Nonomura, P. Qin, G. Boschloo, T. Brinck, A. Hagfeldt, L. Sun, *J. Org. Chem.* **2007**, *72*, 9550-9556.

[27] D. Franchi, M. Calamante, G. Reginato, L. Zani, M. Peruzzini, M. Taddei, F. Fabrizi de Biani, R. Basosi, A. Sinicropi, D. Colonna, A. Di Carlo, A. Mordini, *Tetrahedron* **2014**, *70*, 6285-6295.

[28] A. Dessì, M. Calamante, A. Mordini, M. Peruzzini, A. Sinicropi, R. Basosi, F. Fabrizi de Biani, M. Taddei, D. Colonna, A. Di Carlo, G. Reginato, L. Zani, *Chem. Commun.* **2014**, *50*, 13952-13955.

[29] A. Dessì, M. Calamante, A. Mordini, M. Peruzzini, A. Sinicropi, R. Basosi, F. Fabrizi de Biani, M. Taddei, D. Colonna, A. di Carlo, G. Reginato, L. Zani, *RSC Adv.* **2015**, *5*, 32657-32668.

[30] B. C. Thompson, Y.-G. Kim, T. D. McCarley, J. R. Reynolds, *J. Am. Chem. Soc*. **2006**, *128*, 12714-12725.

[31] A. Leliège, J. Grolleau, M. Allain, P. Blanchard, D. Demeter, T. Rousseau, J. Roncali, *Chem. Eur. J.* **2013**, *19*, 9948–9960.

[32] J. Tauc, *Mater. Res. Bull.* **1968**, *3*, 37-46.

[33] C. Coluccini, N. Manfredi, M. M. Salamone, R. Ruffo, M. Grazia Lobello, F. De Angelis, A. Abbotto, *J. Org. Chem.* **2012**, *77*, 7945-7956.

[34] J. O. M. Bockris, S. U. M. Khan, *Surface Electrochemistry - A Molecular Level Approach*, Springer US, New York, **1993**.

[35] H. Tian, X. Yang, J. Cong, R. Chen, C. Teng, J. Liu, Y. Hao, L. Wang, L. Sun, *Dyes Pigments* **2010**, *84*, 62-68.

[36] B. Cecconi, N. Manfredi, R. Ruffo, T. Montini, I. Romero-Ocaña, P. Fornasiero, A. Abbotto, *ChemSusChem* **2015**, *8*, 4216-4228.

[37] H. Kisch, D. Bahnemann, *J. Phys. Chem. Lett.* **2015**, *6*, 1907-1910

[38] S. Y. Reece, J. A. Hamel, K. Sung, T. D. Jarvi, A. J. Esswein, J. J. Pijpers, D. G. Nocera, Science **2011**, *334*, 645-648.

[39] G. Carraro, C. Maccato, A. Gasparotto, T. Montini, S. Turner, O. I. Lebedev, V. Gombac, G. Adami, G. Van Tendeloo, D. Barreca, P. Fornasiero, *Adv. Funct. Mater.* **2014**, *24* 372–378.

[40] R. Abe, K. Hara, K. Sayama, K. Domen, H. Arakawa, *J. Photochem. Photobiol. A* **2000**, *137*, 63-69.

[41] Q. Li, Y. Che, H. Ji, C. Chen, H. Zhu, W. Ma, J. Zhao, *Phys. Chem. Chem. Phys.* **2014**, *16*, 6550-6554.

[42] It should be noted that although compound **AD418** is similar to the photosensitizers already reported by Kang and co-workers (see ref. 10), in those cases the effect of hydrophobic alkyl chains placed in the intermediate section of the molecules was not investigated, and H_2 production was performed under different conditions using another SED (EDTA).

[43] K. Kalyanasundaram, J. Kiwi, M. Grätzel, *Helv. Chim. Acta* **1978**, *61*, 2720-2730.

[44] A.-M. Manke, K. Geisel, A. Fetzer, P. Kurz, *Phys. Chem. Chem. Phys.* **2014**, *16*, 12029-12042.

[45] A. Listorti, B. O'Regan, J. R. Durrant, *Chem. Mater.* **2011**, *23*, 3381-3399.

[46] S. Kundu, A. B. Vidal, M. A. Nadeem, S. D. Senanayake, H. Idriss, P. Liu, J. A. Rodriguez, D. Stacchiola, *J. Phys. Chem. C* **2013**, *117*, 11149-11158.

[47] S. Yang, H. Wang, H. Yu, S. Zhang, Y. Fang, S. Zhang, F. Peng, *Int. J. Hydrogen En.* **2016**, *41*, 3446-3455.

[48] R. A. Rightmire, R. L. Rowland, D. L. Boos, D. L. Beals, *J. Electrochem. Soc.* **1964**, *111*, 242–247

[49] S. C. S. Lai, M. T. M. Koper, *Faraday Discuss.* **2008**, *140*, 399-416.

[50] M. J. Giz, G. A. Camara, *J. Electroanal. Chem.* **2009**, *625*, 117-122.

[51] B. Pierozynski, *Int. J. Electrochem. Sci.,* **2012**, *7,* 4261-4271.

[52] D. Wang, J. Liu, Z. Wu, J. Zhang, Y. Su, Z. Liu, C. Xu, *Int. J. Electrochem. Sci.* **2009**, *4*, 1672-1678.

[53] A. von Weber, E. T. Baxter, S. Proch, M. D. Kane, M. Rosenfelder, H. S. White, S. L. Anderson, *Phys. Chem. Chem. Phys.* **2015**, *17*, 17601-17610.

[54] U. Pal, S. Ghosh, D. Chatterjee, *Transition Met. Chem.* **2012**, *37*, 93-96.

[55] T.-N. Ye, M. Xu, W. Fu, Y.-Y. Cai, X. Wei, K.-X. Wang, Y.-N. Zhao, X.-H. Li, J.-S. Chen, *Chem. Commun.* **2014**, *50*, 3021-3023.

[56] S. M. Unni, L. George, S. N. Bhange, R. N. Devi S. Kurungot, *RSC Adv.* **2016**, *6*, 82103-82111.

[57] W. Jones, D. J. Martin, A. Caravaca, A. M. Beale, M. Bowker, T. Maschmeyer, G. Hartley, A. Masters, *Appl. Catal. B* **2017**, *in press*, DOI: 10.1016/j.apcatb.2017.01.042.

[58] Y. Pellegrin, F. Odobel, *C. R. Chim.* **2017**, *20*, 283-295, and references therein.

[59] D.V. O'Connor, D. Phillips, *Time Correlated Single Photon Counting*, Academic Press, London, U.K., **1984**.

[60] I. Romero Ocaña, A. Beltram, J. J. Delgado Jaén, G. Adami, T. Montini, P. Fornasiero, *Inorg. Chim. Acta* **2015**, *431*, 197–205.

10.1002/cssc.201701707

Entry for the Table of Contents (Please choose one layout)

FULL PAPER

Photocatalytic H_2 production mediated by organic dye-sensitized Pt/TiO_2 nanopowders was investigated using TEOA and, for the first time, EtOH as sacrificial electron donors (SEDs). Results indicate that good compatibility between individual dye properties and the particular SED used in the experiment is vital to maximize catalytic efficiency.

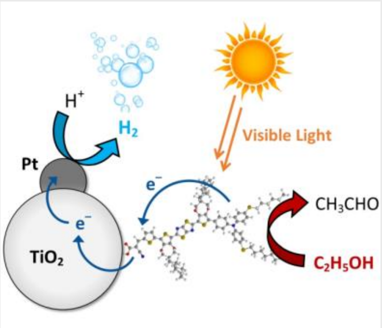

A. Dessì, M. Monai, M. Bessi, T. Montini, M. Calamante, A. Mordini, G. Reginato, C. Trono, P. Fornasiero, L. Zani**

Page No. – Page No.

Towards Sustainable H_2 Production: Rational Design of Hydrophobic Triphenylamine-based Dyes for Sensitized Ethanol Photoreforming